

TURBULENCE AND GALACTIC STRUCTURE

Bruce G. Elmegreen

IBM Research Division, T.J. Watson Research Center, 1101 Kitchawan Road, Yorktown Hts., NY 10598, USA

Abstract Interstellar turbulence is driven over a wide range of scales by processes including spiral arm instabilities and supernovae, and it affects the rate and morphology of star formation, energy dissipation, and angular momentum transfer in galaxy disks. Star formation is initiated on large scales by gravitational instabilities which control the overall rate through the long dynamical time corresponding to the average ISM density. Stars form at much higher densities than average, however, and at much faster rates locally, so the slow average rate arises because the fraction of the gas mass that forms stars at any one time is low, $\sim 10^{-4}$. This low fraction is determined by turbulence compression, and is apparently independent of specific cloud formation processes which all operate at lower densities. Turbulence compression also accounts for the formation of most stars in clusters, along with the cluster mass spectrum, and it gives a hierarchical distribution to the positions of these clusters and to star-forming regions in general. Turbulent motions appear to be very fast in irregular galaxies at high redshift, possibly having speeds equal to several tenths of the rotation speed in view of the morphology of chain galaxies and their face-on counterparts. The origin of this turbulence is not evident, but some of it could come from accretion onto the disk. Such high turbulence could help drive an early epoch of gas inflow through viscous torques in galaxies where spiral arms and bars are weak. Such evolution may lead to bulge or bar formation, or to bar re-formation if a previous bar dissolved. We show evidence that the bar fraction is about constant with redshift out to $z = 1$, and model the formation and destruction rates of bars required to achieve this constancy. Bar dissolution has to be accompanied by rapid bar reformation to get the constant bar fraction. This reformation is consistent with numerical simulations by Block et al. (2002), but it may not be possible according to models by Regan & Teuben (2004). The difference between these simulations is partly the result of a difference in the two models for gas viscosity, which depends on the approximations used to represent turbulence. In the Regan & Teuben model, a constant observed bar fraction implies that bars do not dissolve significantly in a Hubble time.

Keywords: Turbulence, Interstellar Matter, Star Formation, Galactic Structure, Galaxy Bars

to appear in: Penetrating Bars through Masks of Cosmic Dust: The Hubble Tuning Fork strikes a New Note, Eds., K. Freeman, D. Block, I. Puerari, R. Groess, Dordrecht: Kluwer, in press (presented at a conference in South Africa, June 7-12, 2004)

1. Introduction

Interstellar turbulence plays a major role in the structure and dynamics of interstellar gas, and through its influence on star formation, energy dissipation, and viscosity, has a strong impact on galactic structure. Conversely, galactic structure has an impact on turbulence through the energy that comes from spiral instabilities. A recent review of ISM turbulence is in Elmegreen & Scalo (2004) and Scalo & Elmegreen (2004), and a review of star formation in a turbulent medium is in Mac Low & Klessen (2004).

Interstellar turbulence is difficult to model numerically because a large number of resolution elements are required and there are many terms in the equations. For example, Wada et al. (2002) simulated the inner regions of a 2D disk with self gravity, star formation and supernovae, but no magnetic fields. Shukurov et al. (2004) did a 3D simulation with magnetic fields but no gravity. de Avillez & Breitschwerdt (2004) modeled the vertical structure in a galaxy disk at high resolution.

Several points about ISM turbulence are important for this discussion.

(1) The cool neutral medium is usually supersonic on scales larger than several tenths of a parsec and therefore easily compressed in the converging parts of turbulent flows.

(2) The magnetic field follows and resists this compression, although shocks still occur parallel and perpendicular to the field if the gas speed exceeds the Alfvén speed. When the gas moves slower than this, compression occurs mostly in the parallel direction (e.g., Ostriker, Stone & Gammie 2001).

(3) The energy density of motion in supersonic turbulence dissipates rapidly, in about the crossing time of any flow region, regardless of the presence of a magnetic field (Mac Low et al. 1998; Stone, Ostriker & Gammie 1998; Mac Low 1999; Padoan & Nordlund 1999). This implies that bulk ISM velocities should dissipate in ~ 20 My, the flow time over the disk thickness, and on much shorter times for smaller scales. Consequently, ISM motions require constant stirring on the scale of the disk thickness.

(4) Clouds, cloud cores, and other ISM structures, as well as whole star-forming regions, should maintain their form and activity for only one or two crossing times if their gas is supersonically turbulent. Clouds or cores where thermal motions dominate might live much longer if they are not unstable to gravitational collapse.

A crossing time corresponds to the shortest possible formation time for stars, clusters, associations, and star complexes. Short is in a relative sense though, not in the sense of an absolute number of years, because the bigger structures take longer absolute times to form. Short formation times are measured directly by the duration of star formation (Elmegreen & Efremov 1996; Ballesteros-Paredes, Hartmann & Vázquez-Semadeni 1999; Elmegreen 2000; Hartmann et al. 2001). It follows that internal energy sources are not required to generate the turbulence observed in most clouds. It can usually be attributed to residual energy left over from the compressive processes that formed the clouds, in addition to gravitational binding energy for the collapsing clouds.

Turbulence in *incompressible* flows can span a wide range of velocities and spatial scales. Fast flows on large scales contain slower flows on smaller scales in a cascade that extends all the way from the energy source down to the energy dissipation in molecular collisions. The power spectrum of squared-velocity in one dimension is close to a power law with an index of $-5/3$ for incompressible flows. This was predicted by Kolmogorov (1941) using energy conservation for a downward cascade. The power spectrum of any squared quantity in 1D is the energy spectrum, $E(k)dk$. The energy spectrum is related to the power spectrum $P(k)dk$ observed in higher dimensions D by $E(k)dk = P(k)dk^D$. This picture of a uniform cascade of turbulent energy in space and velocity involves interactions between velocity wavenumbers that are comparable in magnitude – sometimes referred to as local in wavenumber space. This is because large flows or eddies carry along the smaller eddies, in a Galilean invariant sense, without much interaction between the two. Possible complications from non-locality in incompressible turbulence were discussed by Zhou, Yeung & Brasseur (1996).

(5) Supersonic ISM turbulence has non-local energy flow in shock fronts when it carries energy from large scales directly to the atomic mean free path without passing through an intermediate cascade. Energy in supersonic turbulence also gets transferred between solenoidal, compressional, and thermal modes. Boldyrev (2002) predicted an energy spectrum $E(k) \sim k^{-1.74}$ by assuming MHD turbulence is mostly solenoidal (incompressible) with Kolmogorov scaling, and that the most dissipative structures are shocks (see also Boldyrev, Nordlund & Padoan 2002). Cho & Lazarian (2002) separated the shear (incompressible) and the fast and slow compressible modes in a compressible MHD simulation for the case where thermal pressure is much less than magnetic pressure and found little coupling between the incompressible and compressible parts. For purely solenoidal driving, the shear modes had $k^{-5/3}$ energy scaling for velocity and field, as did the density in the weakly coupled slow mode; the weakly coupled fast mode had $k^{-3/2}$ scaling for velocity, magnetic field, and density. Cho & Lazarian (2003) got the same result for the high pressure case.

(6) Supersonic turbulence can also carry energy from small to large scales, as when an explosion produces a large moving shell.

There are many observations of power spectra for ISM column densities and emission fluctuations (see review in Elmegreen & Scalo 2004). They are all approximately power laws with a slope of around -3 ± 0.2 in 2D maps (i.e., slightly steeper than the 2D Kolmogorov slope of $-8/3$). These power laws often extend from the smallest observable scale to the largest, including the whole galaxy if data are available, as for the HI maps of the SMC (Stanimirovic 1999) and LMC (Elmegreen, Kim, & Staveley-Smith 2001). Local HI emission (Dickey et al. 2001) shows the same structure.

Another important difference between the Kolmogorov model of incompressible turbulence and ISM turbulence is the spatial scale for energy input. In the Kolmogorov model, kinetic energy is applied on some large scale and it causes motions on smaller and smaller scales down to the dissipation length, where the advection rate equals the dissipation rate. In contrast,

(7) ISM motions are stirred frequently and over a very wide range of scales by various types of sources.

On large scales, turbulent energy comes from gravitational and magnetic instabilities, gravitational scattering of nearby clouds, cloud-disk impacts, and superbubbles. On intermediate scales it comes from supernovae, stellar winds, and expanding HII regions. On small scales it comes from low mass stellar winds and gravitational wakes, Kelvin-Helmholtz and other fluid instabilities, and possibly cosmic-ray streaming, although that is probably more important in the ionized medium. Reviews of these processes are in Norman & Ferrara (1996), Mac Low & Klessen (2004), and Elmegreen & Scalo (2004).

For the ISM, energy sources are so close together in time and space that the gas reaction to one source of energy is usually interrupted by another source before the first fully dissipates. For example, a swing-amplified gravitational instability might make a spiral arm and drive motions in the gas on a kpc scale, but star formation inside this arm and self-gravity inside smaller clouds will drive other motions on smaller scales before the original spiral arm energy is dissipated. This driving energy is not necessarily partitioned into a power law in wavenumber space, or at least not the same power law as the turbulent energy it creates. Thus the resulting power law for ISM turbulent energy will in general be a combination of the distribution of scales for the input energy and the distribution of scales for the non-linear gas reaction to this input. Only on scales much smaller than the smallest input, or for times that are significantly removed from the last input event, can a state of pure gas turbulence be realized. This might apply to scintillation observations, for example (see Scalo & Elmegreen 2004).

One observational implication of this multi-scale agitation is that the ISM often resembles a network of shells or spiral arm fragments with most of the

cool neutral matter along the shells or in the arms. Shells dominate the structure of the LMC (Kim et al. 1999) and other small galaxies (e.g., Ho II: Puche et al. 1992) where shear is low, while shells (Brand & Zealey 1975; Heiles 1979) and spiral arms tend to dominate the structure when shear is high (high shear rate means in comparison to the shell growth rate or the instability growth rate). The shells in the LMC are even somewhat self-similar, spanning a range of scales over a factor of at least 10 (Elmegreen, Kim, & Staveley-Smith 2001). Flocculent spiral arms are self-similar too, combining into a power law power spectrum (Elmegreen, Elmegreen, & Leitner 2003). Thus shells and spiral arms are intimately related to turbulence because both are drivers of turbulence and both are structural reactions to turbulence (Wada, Spaans, & Kim 2000).

There is a similar multi-scale aspect to energy *dissipation* in the ISM, making it different again from incompressible turbulence:

(8) Energy dissipation in the neutral ISM covers a wide range of scales, ranging from decompression regions downstream of spiral arms or in disk-halo outflows, to ion-neutral slip viscosity in all structures with field strength gradients, to continuous dissipation in smooth magnetic shocks, to thin hydrodynamic shocks. A similar range of scales is involved with dissipation of turbulence in the ionized component (see review in Elmegreen & Scalo 2004).

The wide range of scales for both energy input and dissipation underscores the difference between ISM turbulence and the standard Kolmogorov picture of energy cascade from large scale input to small scale dissipation.

In the next section, we outline several aspects of interstellar turbulence as they are related to galactic structure. Given the current level of uncertainty about the nature of ISM turbulence, our view on many of these issues is rapidly evolving.

2. Turbulence and Star Formation

Stellar and galactic power sources in the ISM compress interstellar gas and form clouds directly, often in shock fronts, while shock-shock collisions and secondary shocks inside these fronts make further structures down to very small scales (0.1 pc or less). The first generation shocks could be from a spiral density wave or swing amplified instabilities, or it could be from an explosion and subsequent shell. The secondary shocks are inside the compressed clouds and in the hot cavities between them. If the overall medium is significantly self-gravitating or if a cloud is significantly self-gravitating, then some of the secondary shocks inside these regions can produce gas that is also significantly self-gravitating, and this gas can collapse into smaller clouds, cloud cores, or stars before the ambient turbulence shears and distorts the region out of existence. A review of these star-formation processes is in MacLow & Klessen

(2004), while simulations are in Gammie et al. (2003), Y. Li et al. (2003), P.S. Li et al. (2004) and elsewhere. A different type of simulation is in papers by Bate and collaborators (e.g., Bate, Bonnell & Bromm 2003), who find collapse in turbulent gas down to very small scales and masses where the optical depth becomes large. Then star formation proceeds upwards in mass from there, as a result of accretion. In either case, cloud turbulence defines the primary cloud structure and self-gravity inside this structure leads to star formation.

An important result of turbulence simulations in isothermal gas, as might apply to molecular cloud cores, is that the probability distribution function (pdf) for density is approximately a log-normal (e.g., Li, et al. 2004), with a power law tail in gravitationally collapsing regions at high density (Klessen 2000). The log-normal indicates that the gas density changes randomly and multiplicatively by successive compressions and rarefactions (Vázquez-Semadeni 1994). When the gas becomes sufficiently self-gravitating, this random, two-directional process stops and the gas density increases monotonically until a star forms. Observations suggest that the point of no return occurs at a density of about 10^5 molecules cm^{-3} . This may be just a coincidence for the local regions that are usually observed, or it may be the result of specific processes that change at this density, promoting collapse. For example, at around 10^5 cm^{-3} , big charged grains start to decouple from the magnetic field, molecules freeze onto grains, and the turbulent speed drops to about the sound speed, making further compressions difficult (see review in Elmegreen 2000).

The density pdf may be integrated over the high density tail to find the volume fraction of gas at high density, f_V . In the log-normal of Wada & Norman (2001), which may be representative of galaxy disks, the volume fraction at a density above 10^5 times the average density is equal to $f_V = 10^{-9}$. Similarly, the mass fraction above 10^5 times the average density is $f_M \sim 10^{-4}$. If turbulence establishes the density sub-structure in clouds, and if gas collapses only at densities greater than 10^5 times the average, then this 10^{-4} should be the fraction of the ISM mass that goes into stars in each turbulent crossing time on the small scale, where the collapse occurs. The star formation rate per unit volume on a galactic scale is then

$$SFR/V = f_V \epsilon \rho_5 (G\rho_5)^{1/2}, \quad (1)$$

where ϵ is the fraction of the gas mass inside a dense clump that goes into a star or stars in a dynamical time, f_V is again the volume fraction of the whole ISM above this density, and ρ_5 is the high density where collapse becomes inevitable, taken here to be $10^5 \mu \text{ cm}^{-3}$ for mean molecular weight $\mu \sim 4 \times 10^{-24}$ g. The basic rate of star formation used in this equation is the dynamical rate from gravity, $(G\rho)^{1/2}$. Star formation usually proceeds at about this rate with fairly high efficiency in a cloud core, $\epsilon \sim 0.3 - 0.5$ (e.g., Matzner &

McKee 2000). Setting the density at 10^5 cm^{-3} and using $f_V = 10^{-9}$ gives a galaxy wide average star formation rate of $10^{-5} M_\odot \text{ pc}^{-3} \text{ My}^{-1}$.

This is the same rate that comes from the Kennicutt (1998) observation, which gives a star formation rate per unit area of $SFR/A \sim 0.033\Sigma\Omega$ for mass column density Σ and galaxy rotation rate Ω . This observation applies to all galaxies in Kennicutt's survey, to the inner parts of these galaxies and to starburst galaxies. To convert this to a rate per unit volume, we use the fact that the local density is always about the tidal density, $\rho_{tid} = 3\Omega^2 / (2\pi G)$, assume a flat rotation curve, and assume an exponential disk. Then integrating over the disk from the center to an outer edge at four exponential scale lengths gives an average star formation rate per unit volume of

$$SFR/V \sim 0.012\rho (G\rho)^{1/2} \quad (2)$$

The result for average density $\rho \sim 1\mu \text{ g cm}^{-3}$ is the same as the estimate above, $10^{-5} M_\odot \text{ pc}^{-3} \text{ My}^{-1}$.

This exercise suggests that the star formation rate in essentially all galaxies, averaged over large enough areas, is determined by the available gas (the ρ term) turning into stars on the local dynamical rate, $(G\rho)^{1/2}$, with an efficiency of ~ 0.01 . This low average efficiency is understood for a turbulent medium to be the result of turbulent fragmentation: a small but predictable fraction of the gas is at a density high enough to form stars, which is about 10^5 times the average ρ . The rest of the gas has a density lower than this, making it more easily distorted by random turbulent flows.

Turbulence not only partitions the gas into clumps, but it also locates these clumps in a certain fashion, giving the overall ISM a hierarchical structure with large clumps containing small clumps in many levels of the hierarchy. If stars form in the densest regions of this gas, then they should have the same hierarchical structure. This is widely observed to be the case. Zhang, Fall, & Whitmore (2001) showed that clusters in the Antenna galaxy are correlated in a power-law fashion (i.e., hierarchically clumped together) for scales less than $\sim 1 \text{ kpc}$. Elmegreen & Elmegreen (2001) found fractal structure in the star fields of many galaxies and showed that the fractal dimension is about the same as for the gas. Earlier work by Feitzinger & Braunsfurth (1984), Feitzinger & Galinski (1987), Elmegreen & Efremov (1996), and Efremov & Elmegreen (1998) also found fractal patterns for young stars.

Entire galaxies also have correlated optical structure from a combination of star formation and dust extinction. Power spectra of azimuthal profiles of the optical light from galaxies show power-law forms with slopes comparable to $-5/3$ (Elmegreen, Elmegreen & Leitner 2003), which is the slope for the velocity power spectrum in Kolmogorov turbulence. The power spectrum of the optical light in NGC 5055 is essentially the same as the power spectrum of HI in the LMC, as shown in Figure 1. Models including randomly positioned

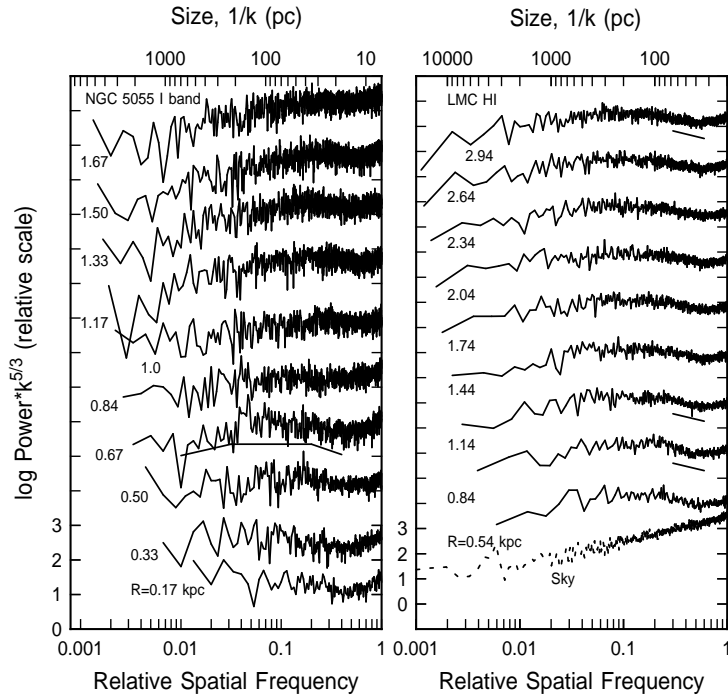


Figure 1. Power spectra of the azimuthal profiles of HI emission from the LMC (right) and optical I-band emission from NGC 5055 (left). The power spectra are multiplied by $k^{5/3}$ to flatten them for easy inspection if they are near the Kolmogorov spectrum of $k^{-5/3}$. The LMC gas and NGC 5055 star formation have remarkably similar power spectra, and power spectra that are also similar to that of incompressible turbulence. This result suggests that star formation distributions are regulated by turbulent processes. (Figure from Elmegreen 2004.)

foreground stars, hierarchically distributed clusters in the galaxy, plus hierarchically distributed field-star light in the galaxy reproduce the observations well (Elmegreen et al. 2003).

Different nomenclature is often applied to various parts of this hierarchy, ranging from star complexes such as Gould's Belt on the largest scales (Efremov 1995) to OB associations and subgroups on smaller scales. These regions are all likely to be part of the same physical processes involving gravitational instabilities, turbulent fragmentation, and direct compression from stellar pressures.

Recall the discussion in the introduction where the driving sources for ISM turbulence were noted to be widespread and overlapping in space and time. This means that shell formation and cloud compression by high pressure events

are sources for turbulence as well as sources for triggering star formation. Star formation operates only in the densest parts of the ISM, and all of these stirring processes occur at much lower densities. Thus the organization to star formation on large scales may not be important for the overall star formation rate. Nevertheless this stirring affects the spatial distribution of the clusters that eventually form, often placing them along the rims of shells or in comet-heads.

Elmegreen (2002) summarized this dichotomy by saying that turbulence fragments the gas into dense pieces, but these pieces are constantly buffeted and compressed by the same energy sources that drive this turbulence, triggering star formation in a high fraction of cases. As long as this turbulence makes a regular density pdf, the overall star formation rate is determined in large part by the fraction of the gas at high density. The rate that comes from this fraction is about the same as the large-scale rate that comes from gravitational instabilities at the average density of the ISM. The details of the stirring and local triggering processes are relatively unimportant (see also Wada & Norman 2001).

Another way to visualize this is to consider the bottleneck to star formation in galaxies. The rate-limiting processes are all on the large scale where the density is low and the dynamical time long. On this scale, the onset of star formation is primarily by gravitational processes, such as swing-amplified instabilities. However, stars actually form on a much smaller scale. The link between these two scales is provided by turbulence. The small dense clumps made by this turbulence each turn into stars very quickly, and have virtually no consequence, individually, to the processes on the large scale because they represent only a very small fraction of the total gas mass (10^{-4}). However, these small clumps are continuously regenerated by the turbulence on larger scales, forming more stars, and this regeneration continues for the dynamical time on the large scale. In each dynamical time on the large scale, 100 cycles of core regeneration occur, turning $100 \times 10^{-4} = 1\%$ of the gas into stars. This gives the Kennicutt (1998) star formation law for all galactic regions, including starbursts.

3. Turbulence and Disk Accretion

Turbulence produces viscosity, which leads to disk accretion. If the viscous time is proportional to the star formation time, then a gas disk can evolve toward an exponential profile (Lin & Pringle 1987; Yoshii & Sommer-Larsen 1989; Saio & Yoshii 1990; Gnedin, Goodman & Frei 1995; Ferguson & Clarke 2001). This process does not appear to be self-regulating, however. If the viscous time is much less than the star formation time, then there is the type of feedback that is needed for regulation: the disk accretes, the density increases, the star formation rate per unit area increases, and the two rates come into

balance. However, if the viscous time is much greater than the star formation time, then there is no feedback: star formation simply removes the gas by turning it into stars, and the accretion stops. Modern cosmology simulations produce exponential disks from the start (Robertson et al. 2004), without needing an evolutionary process involving accretion and star formation, so viscous production of exponential disks is not necessary.

Disk accretion brings gas to the centers of galaxies, leading to bar destruction if the accreted gas mass is large enough (Hasan & Norman 1990; Pfenniger & Norman 1990; Bournaud & Combes 2002; Debattista et al. 2004). Negative torques from viscous accretion outside the bar region are usually overcome by positive bar and spiral arm torques there, which drive a net outflow. Accretion inside the bar region is driven mostly by bar torques, with positive or negative pressure gradients that contribute to these torques. The net accretion rate depends on the energy loss in addition to the torques. This energy loss is uncertain but likely to be rapid. Energy from star formation can restore some of the internal gas energy downstream, and the pressure from this energy, pushing against the front side of the spiral or bar, can restore some of the lost angular momentum.

The equation of motion for a fluid has a contribution to the time derivative from viscosity that can be written $\nu \nabla^2 v$, from which the accretion time may be estimated to be D^2/ν for inverse gradient distance D . The viscous coefficient ν is from turbulence rather than molecular collisions, and its value is unknown. If it can be represented by the product of a length and a speed, $\nu = \lambda c$, then λ might be the outer scale for the correlated motions and c the rms turbulent speed on that scale. Both of these quantities are highly uncertain, particularly because the ISM may have a 3D type of turbulence on scales smaller than the disk thickness and a 2D turbulence on larger scales (Elmegreen, Kim, & Staveley-Smith 2001). A good guess for λ might be the disk thickness itself, in which case $\lambda \sim 200$ pc. Then the velocity dispersion is the rms speed of most of the gas mass, which is ~ 5 km s⁻¹. These parameters give an accretion time over distance D :

$$t_{acc} \sim \frac{10 \text{ Gy } (D/\text{kpc})^2}{(\lambda/200 \text{ pc}) (c/5 \text{ km s}^{-1})}. \quad (3)$$

This is a very long time, even longer if we consider that the real length for the disk gradient is the exponential scale length, which is typically several kpc. Numerical simulations of galaxy disks with gas represented by discrete particles that have longer mean free paths than the disk thickness (averaged over an orbit) can have shorter viscous accretion times than this, possibly leading to spurious effects.

Given the likely small value for the viscous coefficient, disk accretion is dominated by gravitational torques produced in spiral arms and bars. Spirals

and bars transfer angular momentum from the inner disk to the outer disk (Lynden Bell & Kalnajs 1972). Bars produce accretion in the inner part, often to a nuclear ring (Regan & Teuben 2004), and outflow in the outer part, often to an outer resonance ring (Schwarz 1981). Bars are much stronger perturbers than spirals because typically only barred galaxies have outer resonance rings (Buta & Combes 1996). The lack of outer resonance rings in non-barred galaxies seems to imply that these galaxies never had a significant bar in their past. This may imply there are relatively few galaxies that have dissolved bars (see Section 1.4).

4. Turbulence, Viscosity, and Bar Dissolution

The evolution of galaxies over a Hubble time has been studied extensively by simulations but has only recently been observed directly through deep images with the Hubble Space Telescope. Young galaxies often appear physically small and at high restframe surface brightness (Bouwens & Silk 2002), although cosmological dimming allows us to see only the highest surface brightness members of a sample. Galaxies with normal sizes are also present at high z (Simard et al. 1999; Ravindranath et al. 2004). Of interest is the process of galaxy growth and the redistribution of mass inside galaxies during growth. Turbulent viscosity and dissipation play important roles in this redistribution.

Chain galaxies (Cowie, Hu, & Songalia 1995) are interesting because they appear to be unique to high z . They are linear structures with several large bright clumps and no exponential disk or bulge. If they are edge-on disk galaxies (Dalcanton & Schectman 1996; Reshetnikov, Dettmar, & Combes 2003; Elmegreen, Elmegreen, & Sheets 2004a; Elmegreen, Elmegreen, & Hirst 2004b), then their local analogues do not have clumps that extend nearly as far in the vertical direction (e.g., Hoopes, Walterbos, & Rand 1999). The large clump size implies high-speed turbulent motions if the clumps are self-gravitating. The lack of spirals in the face-on counterparts implies that turbulence dominates shear during star formation (Elmegreen, et al. 2004b).

Figure 2 shows three galaxies in the deep field of the Tadpole galaxy (Tran et al. 2003) where we found 69 chain galaxies with three or more giant clumps (as shown on the left in the figure), 58 other linear structures with one or two clumps, and 87 tight clusters of clumps that looked like face-on versions of the chain galaxies (as shown in the middle and right frames of the figure). None of these objects have exponential disks or bright red clumps in their centers that could be bulges. The colors and magnitudes of the clumps and of the whole galaxies in these samples are all about the same, and the distribution of the width-to-length ratio is flat down to a lower limit of ~ 0.2 . Such a flat distribution is appropriate for circular disks and similar to that for local spiral galaxies in the RC3 (de Vaucouleurs et al. 1991; Elmegreen et al. 2004b). The

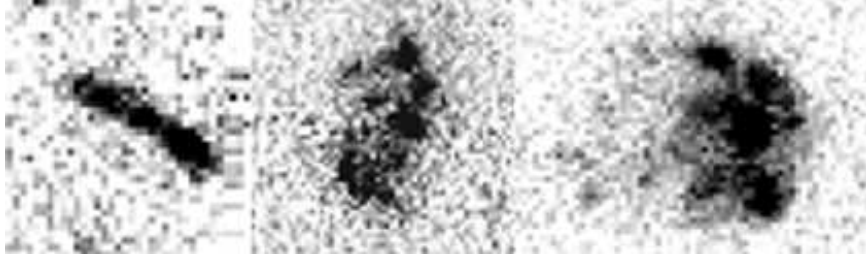


Figure 2. Three high-redshift galaxies from the background field of the Tadpole galaxy are juxtaposed to suggest that chain galaxies (like that on the left) are edge-on versions of clump clusters (like that on the right). This projection is confirmed by the distribution of width-to-length ratios, which is flat as in normal disk galaxies. Neither chains nor clump clusters have exponential disks or prominent red bulges near their centers. Irregular high- z galaxies like this have giant blue clumps that suggest star formation occurred in gas rich disks with large turbulent speeds, comparable to several tenths of the rotation speed. Turbulence in young galaxies could be the result of high galactic accretion rates. (From Elmegreen et al. 2004b.)

implication of these results is that clump-clusters are probably face-on versions of chain galaxies.

The giant clumps in these galaxies are blue and likely to be star-forming regions. Their diameters are ~ 500 pc and they are spaced from each other by several kpc, which is several tenths of the disk diameter. The fact that there are just a few giant clumps per galaxy, along with their dominance of the disk light and the lack of obvious spiral arms, suggests they formed by gravitational instabilities in a medium that is mostly gas and has a relatively high turbulent speed (Noguchi 1999; Immeli et al. 2003, 2004). If we set the Jeans length $1/k_J = c^2/(\pi G\Sigma)$ equal to $1/4$ the galaxy radius, R , for gas surface density Σ , then we need a turbulent speed $c \sim 2V (\Sigma/\Sigma_T) \sim 0.3V$ to $0.5V$ for orbit speed V , where Σ_T is the total effective surface density, including dark matter, that contributes to the rotation. At this turbulent speed, the instability time is comparable to the orbit time and collapsing regions should be spun up by Coriolis forces unless there is a magnetic field in the disk. The brightness of the clumps compared to the underlying disk suggests they are among the first generations of star formation. Presumably some will eventually merge to form an exponential disk or a bulge (Noguchi 1999).

The origin of the turbulence in these galaxies is not clear. Shells or other reactions to star formation are not evident, so most of the turbulent energy may come from the galaxy formation process itself.

Barred galaxies at high z are also prominent in this field. We found 22 clearly barred galaxies out to $z = 1$, complete with grand design spiral arms, bulges, and exponential disks. There were also another 21 galaxies that looked



Figure 3. The Hubble Space Telescope Advanced Camera for Surveys field of the Tadpole galaxy (Tran et al. 2003) is shown in two successive stages of blow-ups revealing normal-looking barred galaxies. This field contains 22 clear barred galaxies like this and 21 additional barred galaxies that are so small their bars show up mostly as inner twists in isophotal contours. The abundance of bars at high z is important for studies of bar dissolution following gas accretion. (for higher resolution, see the jpg version in astro-ph.)

barred on contour plots, which showed an inner isophotal twist. The bar fraction was determined as a function of the ratio of axes and compared with the local bar fraction. Bars were less prominent at high inclinations, more so than local bars at equally high inclinations; the difference is probably the result of poor resolution for the distant bars. We estimated that perhaps twice as many bars were lost to inclination effects at high z than locally. The bar fraction was also determined as a function of z using photometric redshifts from Benitez et al. (2004). This fraction is about constant out to $z \sim 1$ and equal to 0.2 to 0.3. Corrected for inclination, the bar fraction is about the same as the local

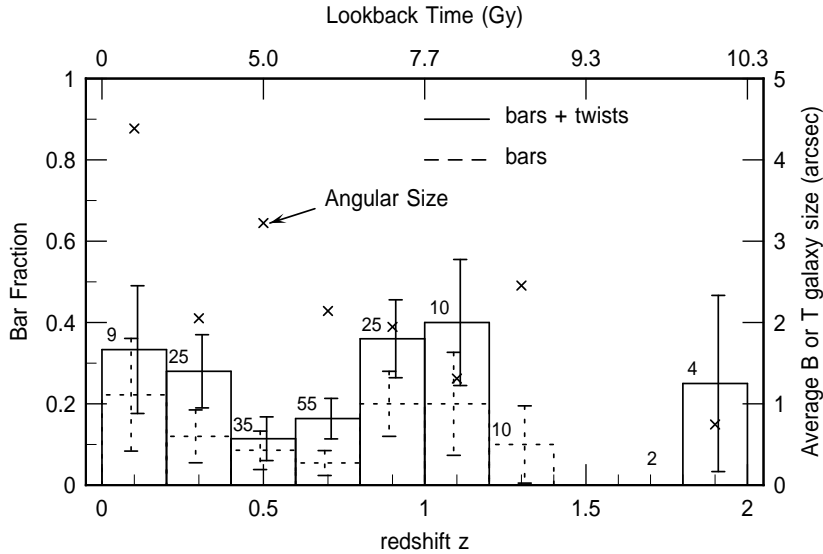


Figure 4. The bar fraction is shown as a function of redshift z for galaxies in the Tadpole field. The solid line histograms are for all bars in the sample, including those which show up only on contour plots. The dashed lines are for the clearest cases of bars. The bar fraction is about constant, suggesting either that bar dissolution is unimportant or bars regenerate relatively quickly once they dissolve. Bar regeneration implies that accreted gas in the outer disk can make its way to the center where it can drive a new bar instability, according to Block et al. (2002). Such accretion without a bar depends on turbulent viscosity and on gravitational torques from spiral arms. (From Elmegreen et al. 2004c.)

fraction, which is ~ 0.4 in B band depending on Hubble type (Elmegreen et al. 2004c). Figure 3 shows two bars in successive blow-ups of the Tadpole field. Figure 4 shows the bar fraction as a function of redshift.

We suggested that a constant bar fraction with z over the last ~ 8 Gy (out to $z = 1$) offers no evidence for bar dissolution over a Hubble time (Elmegreen et al. 2004c). If bars dissolved, then they had to reform, as suggested by Block et al. (2002). However, if non-merger interactions preferentially formed bars, rather than destroyed them (Noguchi 1987; Gerin, Combes & Athanassoula 1990; Berentzen et al. 2004), and if such interactions were more frequent in the past because of the higher galaxy density, as is likely, then the bar formation rate was higher in the past. To maintain a near-constant bar fraction, this means either that the dissolution rate had to be much higher in the past, or that most bars formed early in the Universe and did not dissolve. Regan & Teuben (2004) suggest, for example, that gas accretion in a bar stops at an ILR ring and does not get to the center, in which case the bar would not dissolve.

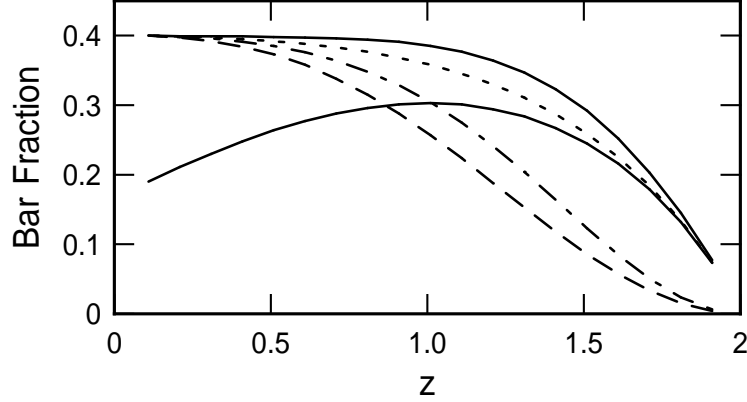


Figure 5. A simple model of bar formation and destruction by various processes is shown to illustrate how prompt bar reformation following internal dissolution can maintain a constant bar fraction out to $z \sim 1$. The dotted line forms bars by galaxy interactions from $z = 2$ to today and has no bar dissolution. The dashed line has bar formation by internal processes with a rate that increases with time at first and then decreases exponentially with an e-folding time of 0.1 Hubble time. The dot-dashed line has the same internal process with a bar dissolution rate proportional to the formation rate. The solid line with a constant bar fraction out to $z = 1$ includes all three processes. All of these examples were tuned to give a bar fraction of 0.4 today. The solid line with a bar fraction that increases out to $z = 1$ has bar formation by interactions and bar dissolution by internal processes with a time scale of 10 Gy. Faster dissolution makes the rise to $z = 1$ larger. This latter case illustrates that even a small amount of bar dissolution cannot operate without continuous re-formation if the bar fraction is to be constant out to $z = 1$.

A simple model illustrates how bar dissolution is possible if the dissolution rate is proportional to the internal formation rate and an additional formation rate from collisions is proportional to the square of the co-moving density out to $z = 2$. Suppose bars form by collisions at the rate

$$\mathcal{F}_{col} = \mathcal{I}_0 (1+z)^6 / (1+2)^6 \quad (4)$$

for constant \mathcal{I}_0 . Here we normalize to the rate at $z = 2$. If this were the only bar formation process and there were no bar destruction, then $\mathcal{I}_0 = 0.51 \text{ Gy}^{-1}$ gives a bar fraction of $f = 0.4$ today. Suppose bars also form by internal processes at a rate given by

$$\mathcal{F}_{int}(z) = \frac{\mathcal{F}_0 (t - t_2)}{0.1\tau} e^{(t-t_2)/(0.1\tau)}. \quad (5)$$

This formation rate increases at first and then decreases with an exponential time scale of 0.1 times the age of the Universe, τ ; t_2 is the time at $z = 2$.

If this were the only bar formation process, then $\mathcal{F}_0 = 0.385 \text{ Gy}^{-1}$ gives a bar fraction of $f = 0.4$ today. Finally, suppose the bar destruction rate is proportional to the internal formation rate:

$$\mathcal{F}_{des} = \mathcal{D}_0 \mathcal{F}_{int}. \quad (6)$$

If bars only formed at the internal process with $\mathcal{F}_{int} = 0.385 \text{ Gy}^{-1}$, and if $\mathcal{D}_0 = 1$, then the final bar fraction would be 0.32 with 9% of all formed bars having been destroyed.

To solve for the bar fraction f we use the equation

$$\frac{df}{dt} = \mathcal{F}_{col}(1 - f) + \mathcal{F}_{int}(1 - f) - \mathcal{F}_{des} * f. \quad (7)$$

We solve this numerically using the conversion from t to z in a standard Λ CDM Universe (see formulae in Elmegreen et al. 2004c). The results are shown in Figure 5 for several parameter values. The dotted line is the bar fraction as a function of z with only collisions operating and no destruction using $\mathcal{I}_0 = 0.51 \text{ Gy}^{-1}$. The dashed line is for internal bar formation only, no destruction, and $\mathcal{F}_0 = 0.385 \text{ Gy}^{-1}$. The dot-dashed line is for internal bar formation and destruction with $\mathcal{F}_0 = 0.605 \text{ Gy}^{-1}$ and $\mathcal{D}_0 = 1$. All of these were tuned to give a bar fraction of 0.4 today, as was the model for the top solid line, which has all three processes acting together using $\mathcal{I}_0 = 0.51 \text{ Gy}^{-1}$, $\mathcal{F}_0 = 0.385 \text{ Gy}^{-1}$, and $\mathcal{D}_0 = 1.85$. Only the solid and dotted lines are constant out to $z \sim 1$. For the case with all three processes, the time integral of the destruction rate, which is the last term in equation 7, equals -0.33 , meaning that this fraction of all the galaxies had a bar dissolve. The other solid line in figure 5 is for a case with $\mathcal{I}_0 = 0.51 \text{ Gy}^{-1}$, no internal formation ($\mathcal{F}_0 = 0$), and a constant destruction rate with $\mathcal{F}_{des} = 0.1 \text{ Gy}^{-1}$. This last example illustrates how even a small amount of bar destruction (i.e., with a bar dissolution timescale of 10 Gy) and no reformation gives a noticeably rising bar fraction out to $z = 1$.

5. Conclusions

Turbulence is related to galactic structure through the star formation rate and morphology and through viscous forces and ISM energy dissipation. ISM turbulence is a complicated process involving thermal and magnetic pressures plus self-gravity, with frequent and multi-scale energy input and dissipation. Between bursts of energy input and when self-gravity is unimportant, MHD turbulence has several properties that carry over from Kolmogorov turbulence, including the power spectrum of the incompressible part of the flow (the shear or solenoidal part).

Star formation is not just the result of gravitational collapse in a turbulent medium because many sources of pressure, such as HII regions and super-

novae, make clouds independently of turbulence and compress the turbulence-made clouds further, triggering additional star formation. A high fraction of all star formation may be triggered in this way. Inside cloud cores, turbulent compression and self-gravity may dominate stellar compression. Also, during the formation of spiral arms by gravitational instabilities and the formation of giant molecular clouds by turbulence and self-gravity, stellar pressures may be unimportant because they are relatively rare on these scales.

Long-term disk evolution also depends on turbulence through its effect on gas viscosity. Turbulent viscosity should be much smaller than simulated viscosity with sticky particles unless the particle collisions are frequent and highly dissipative. Turbulent dissipation in the ISM is so rapid that the entire energy content on the scale of the disk thickness has to be replaced every few disk crossing times. There are apparently enough energy sources with close enough spacings to do this.

When strong bars or spirals are present, global disk accretion is dominated by gravitational torques from these objects and by torques at galactic shock fronts. Accretion by turbulent viscosity is much slower. The appearance of bars at high z with rather normal abundance among disk galaxies suggests either that bars formed early in the Universe and were not easily destroyed, as suggested by Regan & Teuben (2004), or that the bars which were destroyed were promptly replaced by new bars, as suggested by Block et al. (2002). An important difference between these two simulations is the treatment of viscosity. The appearance of irregular galaxies with giant star-forming regions suggests that turbulent velocities were large during the first Gigayear in a galaxy's life.

Acknowledgments

B.G.E. acknowledges support from NSF Grant AST-0205097. Helpful discussions with Debra Elmegreen are appreciated.

References

- Athanassoula, F. 1984, *Phys.Reps.*, 114, 319
- de Avillez, M.A., Breitschwerdt, D. 2004, *Astroph. Sp. Sci.* 289, 479
- Ballesteros-Paredes, J., Hartmann, L., Vázquez-Semadeni, E. 1999, *ApJ*, 527, 285
- Bate, M.R., Bonnell, I.A., Bromm, V. 2003, *MNRAS*, 339, 577
- Benitez, N. et al. 2004, *ApJS*, 150, 1
- Berentzen, I., Athanassoula, E., Heller, C.H., Fricke, K.J. 2004, *MNRAS*, 347, 220
- Bertin G., Lin C.C., Lowe S.A. & Thurstans R.P. 1989, *ApJ*, 338, 78
- Block, D. L., Bournaud, F., Combes, F., Puerari, I., & Buta, R. 2002, *A&A*, 394, L35
- Boldyrev, S. 2002, *ApJ*, 569, 841
- Boldyrev, S., Nordlund, A., & Padoan, P. 2002, *Phys. Rev. Lett.*, 89, 031102
- Bournaud, F., & Combes, F. 2002, *A&A*, 392, 83

- Bouwens, R., & Silk, J. 2002, *ApJ*, 568, 522
- Brand, P.W.J.L., & Zealey, W.J. 1975, *A&A*, 38, 363
- Buta, R.C. & Combes, F. 1996, *Fundam. Cos. Phys.*, 17, 95
- Cho, J., Lazarian, A. 2002, *Phys. Rev. Lett.*, 88, 245001
- Cho, J., Lazarian, A. 2003, *MNRAS*, 345, 325
- Cowie, L., Hu, E., & Songalia, A. 1995, *AJ*, 110, 1576
- Dalcanton, J.J., & Schectman, S.A. 1996, *ApJ*, 465, L9
- Debattista, V.P., Carollo, C.M., Mayer, L., & Moore, B. 2004, *ApJ*, 604, L93
- Dickey, J.M., McClure-Griffiths, N.M., Stanimirovic, S., Gaensler, B.M., Green, A.J. 2001, *ApJ*, 561, 264
- Efremov, Y.N. 1995, *AJ*, 110, 2757
- Efremov, Y. N., & Elmegreen, B. G. 1998, *MNRAS*, 299, 588
- Elmegreen, B.G. 2000, *ApJ*, 530, 277
- Elmegreen, B.G. 2002, *ApJ*, 577, 206
- Elmegreen, B.G. 2004, in *Star Formation in the Interstellar Medium*, ed. F. Adams, D. Johnstone, D. Lin and E. Ostriker, *Astron. Soc. Pacific Conf. Series*, in press.
- Elmegreen, B.G. & Efremov, Y. 1996, *ApJ*, 466, 802
- Elmegreen, D.M., & Elmegreen, B.G. 2001, *AJ*, 121, 1507
- Elmegreen, B.G., Kim, S., Staveley-Smith, L. 2001, *ApJ*, 548, 749
- Elmegreen, B.G. & Scalo, J. 2004, *ARAA*, 42, in press
- Elmegreen, B.G., Elmegreen, D.M., & Leitner, S.N. 2003, *ApJ*, 590, 271
- Elmegreen, B. G., Leitner, S. N., Elmegreen, D. M., Cuillandre, J.-C. 2003, *ApJ*, 593, 333
- Elmegreen, D.M., Elmegreen, B.G., & Sheets, C.M. 2004a, *ApJ*, 603, 74
- Elmegreen, D.M., Elmegreen, B.G., & Hirst, A.C. 2004b, *ApJ*, 604, L21
- Elmegreen, D.M., Elmegreen, B.G., & Hirst, A.C. 2004c, *ApJ*, 612, in press
- Feitzinger, J.V., & Braunsfurth, E. 1984, *A&A*, 139, 104
- Feitzinger, J. V., & Galinski, T. 1987, *A&A*, 179, 249
- Ferguson, A.M.N., & Clarke, C. J. 2001, *MNRAS*, 325, 781
- Gammie, C.F., Lin, Y.-T., Stone, J.M., & Ostriker, E.C. 2003, *ApJ*, 592, 203
- Gerin, M., Combes, F., & Athanassoula, E. 1990, *A&A*, 230, 37
- Gnedin, O.Y., Goodman, J., & Frei, Z. 1995, *AJ*, 110, 1105
- Immeli, A., Samland, M., & Gerhard, O. 2003, in *Galactic and Stellar Dynamics, Proceedings of JENAM 2002*, ed. C. M. Boily, P. Patsis, S. Portegies Zwart, R. Spurzem & C. Theis, *EAS Publications Series*, Volume 10, p. 199.
- Immeli, A., Samland, M., Gerhard, O., & Westera, P. 2004, *A&A*, 413, 547
- Hartmann, L., Ballesteros-Paredes, J., & Bergin, E.A. 2001, *ApJ*, 562, 852
- Hasan, H., & Norman, C. 1990, *ApJ*, 361, 69
- Heiles, C. 1979, *ApJ*, 229, 533
- Hoopes, C.G., Walterbos, R.A.M. & Rand, R.J. 1999, *ApJ*, 522, 669
- Kennicutt, R.C. 1998, *ApJ*, 498, 541
- Kim, S., Dopita, M.A., Staveley-Smith, L., Bessell, M.S. 1999, *AJ*, 118, 2797
- Klessen, R.S. 2000, *ApJ*, 535, 869
- Kolmogorov, A.N. 1941, *Proc. R. Soc. London Ser. A*, 434, 9
- Li, Y., Klessen, R.S., Mac Low, M.-M., 2003, *ApJ*, 592, 975
- Li, P. S., Norman, M.L., Mac Low, M.-M., Heitsch, F. 2004, *ApJ*, 605, 800
- Lin, D.N.C., & Pringle, J.E. 1987, *ApJ*, 320, L87

- Lynden-Bell, D., & Kalnajs, A.J. 1972, MNRAS, 157, 1
- Mac Low, M.-M., Klessen, R.S., Burkert, A., Smith, M.D. 1998, Phys. Rev. Lett., 80, 2754
- Mac Low, M.-M., 1999 ApJ 524, 169
- Mac Low, M.-M., Klessen, R.S. 2004, Rev. Mod. Phys., 76, 125
- Matzner, C.D., & McKee, C.F. 2000, ApJ, 545, 364
- Noguchi, M. 1987, MNRAS, 228, 635
- Noguchi, M. 1996, ApJ, 514, 77
- Norman, C.A., & Ferrara, A. 1996, ApJ, 467, 280
- Ostriker, E. C., Stone, J. M., Gammie, C.F. 2001, ApJ, 546, 980
- Padoan, P., & Nordlund, A. 1999, ApJ, 526, 279
- Pfenniger, D., & Norman, C. 1990, ApJ, 363, 391
- Puche, D., Westpfahl, Brinks, E., & Roy, J-R. 1992, AJ, 103, 1841
- Ravindranath, S., et al. 2004, ApJ, 604, L9
- Regan, M.W., & Teuben, P.J. 2004, ApJ, 600, 595
- Reshetnikov, V., Dettmar, R.-J., & Combes, F. 2003, A&A, 399, 879
- Robertson, B., Yoshida, N., Springel, V., Hernquist, L. 2004, ApJ, 606, 32
- Saio, H., & Yoshii, Y. 1990, ApJ, 363, 40
- Scalo, J., & Elmegreen, B.G. 2004, ARAA, 42, in press.
- Schwarz, M.P. 1981, ApJ, 247, 77
- Shukurov, A., Sarson, G.R., Nordlund, A., Gudiksen, B., Brandenburg, A. 2004, Astroph. Space Sci., 289, 319
- Simard, L., Koo, D.C., Faber, S. M., Sarajedini, V. L., Vogt, N. P., Phillips, A. C., Gebhardt, K., Illingworth, G. D., & Wu, K. L. 1999, ApJ, 519, 563
- Stanimirovic, S., Staveley-Smith, L., Dickey, J.M., Sault, R.J., Snowden, S.L. 1999, MNRAS, 302, 417
- Stone, J. M., Ostriker, E. C., Gammie, C. F. 1998, ApJ, 508, L99
- Tran, H. et al., 2003, ApJ, 585, 750
- de Vaucouleurs, G., de Vaucouleurs, A., Corwin, H., Buta, R., Paturel, G., & Fouque, P. 1991, Third Reference Catalogue of Galaxies, New York: Springer-Verlag
- Vázquez-Semadeni, E. 1994, ApJ, 423, 681
- Wada, K., Spaans, M., & Kim, S. 2000, ApJ, 540, 797
- Wada, K., Norman, C.A. 2001, ApJ, 547, 172
- Wada, K., Meurer, G., Norman, C.A. 2002, ApJ, 577, 197
- Yoshii, Y., & Sommer-Larsen, J. 1989, MNRAS, 236, 779
- Zhang, Q., Fall, S. M., & Whitmore, B. C. 2001, ApJ, 561, 727
- Zhou, Y., Yeung, P.K., Brasseur, J.G. 1996, Phys. Rev. E, 53, 1261

This figure "elmegreen_fg3.jpg" is available in "jpg" format from:

<http://arxiv.org/ps/astro-ph/0407582v1>